

Molecular *g*-Values, Magnetic Susceptibility Anisotropies and Molecular Electric Quadrupole Moments of Difluoroacetonitrile. A Rotational Zeeman Effect Study

J. Spieckermann, M. Andolfatto, and D. H. Sutter

Abteilung Chemische Physik im Institut für Physikalische Chemie der Universität Kiel

Z. Naturforsch. **42a**, 167–173 (1987); received September 22, 1986

The rotational Zeeman effect of several low *J* rotational transitions of difluoroacetonitrile has been studied under high resolution conditions with a microwave superheterodyne bridge spectrometer. The observed anisotropies in the molecular magnetic susceptibility tensor are discussed within the model of local susceptibilities to derive the magnetic susceptibility tensor of the nitrile group. Comparison with results obtained earlier for acrylonitrile shows significant changes, probably due to electron withdrawal from the CN-group by the neighbouring fluorine atoms.

Introduction

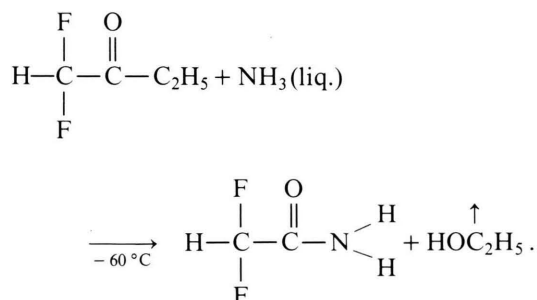
Detailed microwave spectroscopic data for fluorinated acetonitriles have been presented recently [1]. They were obtained by high resolution microwave Fourier transform spectroscopy. In the following we present the results of a rotational Zeeman effect study of difluoroacetonitrile which, by giving information on the magnetic susceptibility tensor of the free molecule and on the diagonal elements of the molecular electric quadrupole moment tensor, further extends our knowledge of the electronic ground state properties of this molecule. The present study is also part of a systematic investigation of substituent effects on the magnetic properties of the C≡N-group.

Experimental

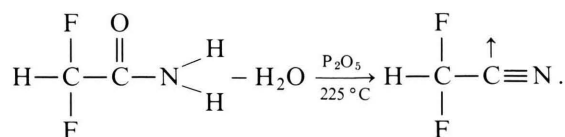
Difluoroacetonitrile was prepared in a two step procedure already used by J. Sheridan and co-workers [1].

In the first step an excess of NH₃ was vacuum distilled into a flask containing ethyldifluoroacetate at liquid N₂ temperature. Then the temperature was raised to approximately –60 °C for reaction. The reactants were thoroughly mixed by magnetic

stirring. At the end of the reaction the excess NH₃ and the C₂H₅OH formed in the reaction were pumped off:



In the second step the difluoroacetamide, a white powder, was mixed with white sand and P₂O₅. The system was evacuated and the temperature was gradually raised to +225 °C for dehydration of the amide.



The product, difluoroacetonitrile, was continuously pumped off and was collected in a trap kept in liquid N₂.

The spectra were recorded with our microwave superheterodyne bridge spectrometer described earlier [2]. Sample pressures used were in the range of 1 to 5 mTorr (0.13 to 0.66 Pa), temperatures were

Reprint requests to Prof. Dr. D. H. Sutter, Abteilung Chemische Physik im Institut für Physikalische Chemie der Universität Kiel, Olshausenstr. 40, D-2300 Kiel, West-Germany.

0340-4811 / 87 / 0200-0167 \$ 01.30/0. – Please order a reprint rather than making your own copy.



Dieses Werk wurde im Jahr 2013 vom Verlag Zeitschrift für Naturforschung in Zusammenarbeit mit der Max-Planck-Gesellschaft zur Förderung der Wissenschaften e.V. digitalisiert und unter folgender Lizenz veröffentlicht: Creative Commons Namensnennung-Keine Bearbeitung 3.0 Deutschland Lizenz.

Zum 01.01.2015 ist eine Anpassung der Lizenzbedingungen (Entfall der Creative Commons Lizenzbedingung „Keine Bearbeitung“) beabsichtigt, um eine Nachnutzung auch im Rahmen zukünftiger wissenschaftlicher Nutzungsformen zu ermöglichen.

This work has been digitalized and published in 2013 by Verlag Zeitschrift für Naturforschung in cooperation with the Max Planck Society for the Advancement of Science under a Creative Commons Attribution-NoDerivs 3.0 Germany License.

On 01.01.2015 it is planned to change the License Conditions (the removal of the Creative Commons License condition “no derivative works”). This is to allow reuse in the area of future scientific usage.

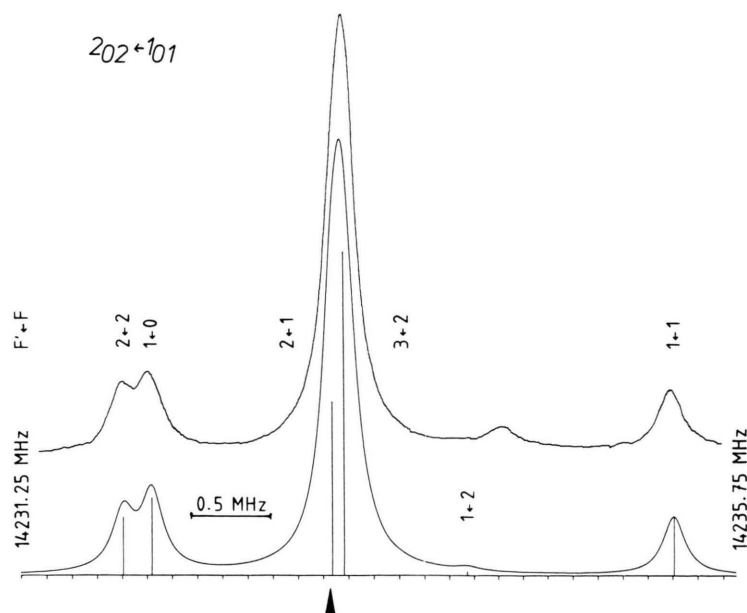


Fig. 1. Zero field quadrupole hyperfine multiplet of the $1_{01} \rightarrow 2_{02}$ rotational transition. Rotational angular momentum, J , and ^{14}N spin angular momentum, I , are coupled due to a nonvanishing intramolecular electric field gradient at the position of the quadrupole nucleus to give a resulting angular momentum, $(J + I) = F$. The satellites are labelled by the corresponding F quantum numbers of the upper and the lower state. Also shown is a computer simulation of the multiplet. It is calculated from the quadrupole coupling constants given in Table 3. Lorentzian line shapes are assumed in this simulation with a full width at half height of 170 kHz. The hypothetical center frequency of the multiplet, which would be the transition frequency in the absence of quadrupole coupling is marked by \blacktriangle . Spin rotation interaction is neglected.

about -60°C . Under these conditions halfwidth at half height were on the order of typically 50 to 75 kHz. Figure 1 shows the zero field ^{14}N quadrupole hyperfine multiplets of the $1_{01} \rightarrow 2_{02}$ rotational transition as an example. Even though the central $F \rightarrow F' = 1 \rightarrow 2$ and $2 \rightarrow 3$ satellites are unresolved, knowledge of their relative intensities makes it possible to derive their individual frequencies with high precision from a line shape analysis such as described in [3].

Results and Analysis

We first measured the zero field ^{14}N hyperfine multiplets for accurate determination of the hypothetical center frequencies [4] of the corresponding rotational transitions in the absence of quadrupole coupling. These multiplet splittings are presented in Table 1. They were also used to fit the ^{14}N quadrupole coupling constants as described for instance in our recent paper on acrylonitrile [5]. The quadrupole coupling constants determined here are in close agreement with those determined in [1]. They are given in Table 3.

In Table 2 we present the observed Zeeman-splittings (compare too Figure 2). They are given with respect to the hypothetical center frequencies, ν_c , of the corresponding zero field hfs multiplet (see

Table 1. Zero field ^{14}N quadrupole hyperfine multiplets observed for the $0_{00} \rightarrow 1_{10}$, $1_{01} \rightarrow 2_{02}$ and the $1_{11} \rightarrow 2_{12}$ rotational transitions. The splittings $\Delta\nu$ are referred to the hypothetical center frequencies of the transitions, which would be observed in the absence of quadrupole coupling. Also given for comparison are the splittings calculated from the optimized quadrupole coupling constants listed in Table 3.

$J_{K_- K_+} \rightarrow J'_{K'_- K'_+}$	$F \rightarrow F'$	Rel. Int.	$\Delta\nu_{\text{exp}}$ [MHz]	$\Delta\nu_{\text{calc}}$ [MHz]
$0_{00} \rightarrow 1_{10}$	$1 \rightarrow 2$	55.5	-0.097	-0.099
	$1 \rightarrow 1$	33.3	+0.494	+0.497
	$1 \rightarrow 0$	11.1	-0.994	-0.994
$1_{01} \rightarrow 2_{02}$	$2 \rightarrow 3$	46.6	+0.089	+0.089
	$1 \rightarrow 2$	25.0	+0.021	+0.018
	$0 \rightarrow 1$	11.1	-1.120	-1.116
	$2 \rightarrow 2$	8.33	-1.301	-1.299
	$1 \rightarrow 1$	8.33	+2.176	+2.177
$1_{11} \rightarrow 2_{12}$	$2 \rightarrow 3$	46.6	0.264	0.262
	$1 \rightarrow 2$	25.0	-1.095	-1.098
	$0 \rightarrow 1$	11.1	+1.692	+1.698
	$2 \rightarrow 2$	8.33	-0.385	-0.377
	$1 \rightarrow 1$	8.33	-0.110	-0.103

above). The diagonal elements of the molecular g -tensor and the anisotropies in the diagonal elements of the magnetic susceptibility tensor were fitted to these splittings as described in [5]. They too are given in Table 3.

For a detailed development of the theoretical background, the reader is referred to [6] and [7]. As

Table 2. Zeeman- ^{14}N quadrupole hfs multiplets observed under $\Delta M_I = 0$, $\Delta M_J = \pm 1$ selection rules for the projection quantum numbers of the ^{14}N -spin and the rotational angular momentum respectively. (The magnetic field very effectively uncouples \mathbf{I} and \mathbf{J} and causes them to precess independently around the field axis, compare too Fig. 5, Ref. [5].) Also listed are the corresponding splittings calculated from the optimized molecular parameters given in Table 3. For details of the calculation see [5] and references cited therein. Relative intensities are given in arbitrary units. “–” indicates relatively weak satellites not included in the fit. “*” indicates satellites, overlapped by a strong and yet unassigned line.

$J K_- K_+ \rightarrow J' K'_- K'_+$ ν_c/MHz	$H/\text{Gauß}$ ΔM_J	M_I	M_J	M'_J	Rel. Int.	$\Delta \nu_{\text{exp}}$ [MHz]	$\Delta \nu_{\text{calc}}$ [MHz]	
$0\ 0\ 0 \rightarrow 1\ 1\ 0$ 14 081.054	$14\ 602$ ± 1	1.0	0	–1	1.98	–0.528	–0.536	–0.008
		–1.0	0	–1	2.00	–0.483	–0.478	0.005
		0.0	0	–1	1.99	–0.206	–0.198	0.008
		1.0	0	1	2.00	*	0.320	*
		–1.0	0	1	1.99	*	0.371	*
		0.0	0	1	1.99	*	0.636	*
$0\ 0\ 0 \rightarrow 1\ 1\ 0$ 14 081.054	$17\ 228$ ± 1	1.0	0	–1	1.99	–0.574	–0.591	–0.017
		–1.0	0	–1	2.00	–0.545	–0.542	0.003
		0.0	0	–1	1.99	–0.267	–0.259	0.008
		1.0	0	1	2.00	*	0.400	*
		–1.0	0	1	1.99	*	0.443	*
		0.0	0	1	1.99	*	0.713	*
$1\ 0\ 1 \rightarrow 2\ 0\ 2$ 14 233.186	$14\ 602$ ± 1	–1.0	1	0	1.94	–	–1.088	–
		1.0	1	0	1.98	–	–0.935	–
		0.0	0	–1	5.79	–0.848	–0.844	0.004
		0.0	–1	–2	11.89	–0.579	–0.574	0.005
		–1.0	–1	–2	12.00	–0.313	–0.315	–0.002
		1.0	–1	–2	11.73	–0.195	–0.236	–0.041
		0.0	0	1	6.00	–0.242	–0.201	0.041
		1.0	0	–1	5.80	–0.147	–0.145	0.002
		–1.0	0	–1	6.08	–0.147	–0.144	0.003
		–1.0	–1	0	1.98	–	–0.006	–
		1.0	–1	0	1.99	–	0.079	–
		0.0	1	2	11.86	0.213	0.210	–0.003
		–1.0	1	2	11.64	0.308	0.307	–0.001
		1.0	1	2	12.00	0.471	0.470	–0.001
		0.0	1	0	1.92	–	0.623	–
		1.0	0	1	6.10	0.657	0.641	–0.016
$1\ 0\ 1 \rightarrow 2\ 0\ 2$ 14 233.186	$17\ 228$ ± 1	–1.0	0	1	5.76	0.657	0.669	0.012
		0.0	–1	0	1.89	–	1.581	–
		–1.0	1	0	1.96	–	–1.098	–
		1.0	1	0	1.99	–	–0.972	–
		0.0	0	–1	5.86	–0.972	–0.955	0.017
		0.0	–1	–2	11.92	–0.660	–0.651	0.009
		–1.0	–1	–2	12.00	–0.396	–0.390	0.006
		1.0	–1	–2	11.80	–0.324	–0.318	0.006
		1.0	0	–1	5.85	–0.236	–0.225	0.011
		–1.0	0	–1	6.06	–0.236	–0.224	0.012
		0.0	0	1	5.99	–0.162	–0.151	0.011
		–1.0	–1	0	1.99	–	0.076	–
		1.0	–1	0	1.99	–	0.152	–
		0.0	1	2	11.90	0.271	0.274	0.003
		–1.0	1	2	11.74	0.398	0.402	0.004
$1\ 1\ 1 \rightarrow 2\ 1\ 2$ 13 339.397	$14\ 602$ ± 1	1.0	1	2	12.00	0.535	0.535	0.000
		0.0	1	0	1.94	–	0.591	–
		1.0	0	1	6.07	0.700	0.702	0.002
		–1.0	0	1	5.83	0.721	0.724	0.003
		0.0	–1	0	1.92	–	1.664	–
		0.0	–1	–2	11.82	–0.940	–0.937	0.003
		–1.0	0	–1	5.88	–0.689	–0.696	–0.007
		1.0	0	–1	5.97	–0.689	–0.682	0.007
		–1.0	1	0	1.96	–	–0.455	–
		1.0	1	0	2.00	–	–0.413	–
$1\ 1\ 1 \rightarrow 2\ 1\ 2$ 13 339.397	$14\ 602$ ± 1	0.0	1	0	2.00	–	–0.359	–
		0.0	1	2	11.81	–0.166	–0.173	–0.007
		–1.0	–1	–2	12.00	–0.166	–0.160	0.006

$J K_- K_+ \rightarrow J' K'_- K'_+$	$H/\text{Gauß}$ ΔM_J	M_I	M_J	M'_J	Rel. Int.	$\Delta \nu_{\text{exp}}$ [MHz]	$\Delta \nu_{\text{calc}}$ [MHz]	$\Delta \nu_{\text{calc}} - \Delta \nu_{\text{exp}}$ [MHz]
$1\ 1\ 1 \rightarrow 2\ 1\ 2$ 13 339.397	17 228 ± 1	1.0	-1	-2	11.67	-0.099	-0.106	-0.007
		-1.0	0	1	5.97	0.105	0.100	-0.005
		1.0	0	1	5.86	0.105	0.111	0.006
		0.0	0	-1	5.83	0.251	0.251	0.000
		-1.0	-1	0	2.00	—	0.421	—
		1.0	-1	0	1.96	—	0.475	—
		0.0	-1	0	2.00	—	0.497	—
		-1.0	1	2	11.75	0.574	0.577	0.003
		1.0	1	2	12.00	0.574	0.620	0.046
		0.0	0	1	5.87	—	1.012	—
		0.0	-1	-2	11.87	-1.021	-1.021	0.000
		-1.0	0	-1	5.91	-0.734	-0.757	-0.023
$1\ 1\ 1 \rightarrow 2\ 1\ 2$ 13 339.397	17 228 ± 1	1.0	0	-1	5.97	-0.734	-0.746	-0.012
		-1.0	1	0	1.97	—	-0.509	—
		1.0	1	0	2.00	—	-0.472	—
		0.0	1	0	2.00	—	-0.416	—
		-1.0	-1	-2	12.00	-0.215	-0.242	-0.027
		1.0	-1	-2	11.77	-0.200	-0.198	0.002
		0.0	1	2	11.86	-0.114	-0.114	0.000
		-1.0	0	1	5.98	0.190	0.180	-0.010
		1.0	0	1	5.88	0.190	0.189	-0.001
		0.0	0	-1	5.90	0.190	0.190	0.000
		-1.0	-1	0	2.00	—	0.501	—
		1.0	-1	0	1.97	—	0.546	—
$1\ 1\ 1 \rightarrow 2\ 1\ 2$ 13 339.397	17 228 ± 1	0.0	-1	0	2.00	—	0.575	—
		-1.0	1	2	11.81	0.638	0.641	0.003
		1.0	1	2	12.00	0.678	0.678	0.000
		0.0	0	1	5.90	—	1.096	—

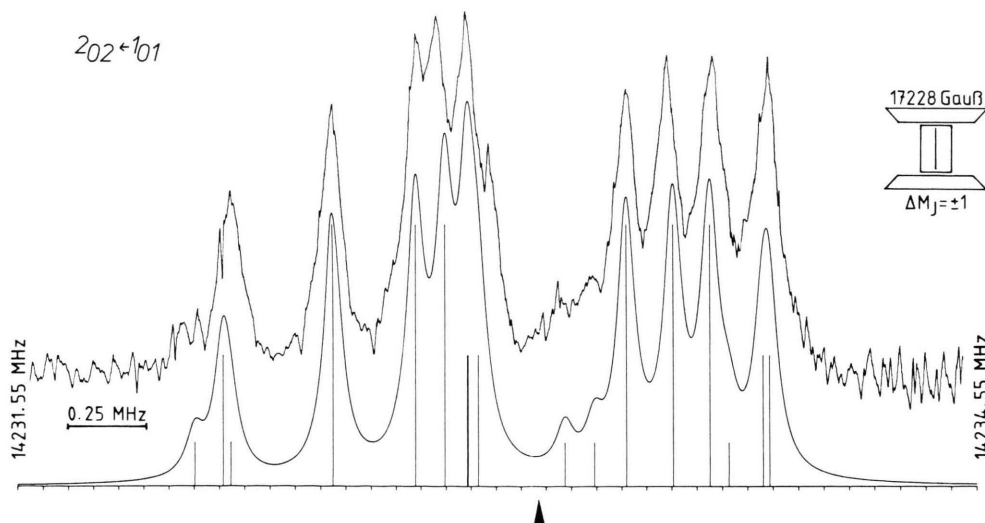


Fig. 2. Multiplet pattern of the $1_{01} \rightarrow 2_{02}$ rotational transition of CHF_2CN observed under $\Delta M_I = 0$, $\Delta M_J = \pm 1$ selection rules in a field of 17 228 Gauß (1.7228 Tesla). The lower trace shows a simulation which was calculated as described in [5] from the molecular parameters listed in Table 3. Lorentzian lineshapes with a full width at half height of 66 kHz were assumed for the satellites.

described in [5] the sign of the g -values was determined unambiguously from intermediate field spectra.

In Table 4 we present molecular parameters, which may be derived from the Zeeman data but which require additional input such as the rota-

tional constants (\rightarrow molecular electric quadrupole moments, and paramagnetic molecular susceptibilities), the molecular structure (\rightarrow anisotropies in the second moments of the electronic charge distribution), and the bulk susceptibility (\rightarrow second moments of the electronic charge distribution and the individual components of the molecular magnetic susceptibility tensor). We note that the only off diagonal elements of the tensors, i.e. Q_{ac} , χ_{ac} , etc. do not follow from our data and are still unknown (all other off diagonal tensor elements are zero by symmetry).

At present only a partial r_0 -structure is available from the work of Ohle and Mäder [8]. It is shown in Figure 3. The corresponding a -, b -, and c -coordinates of the atoms are listed in Table 5. Since no experimental value for the bulk susceptibility was available, we used the additivity scheme developed by Haberditzel [9] to calculate an approximate value from inner shell increments and bond increments. This calculation is presented in Table 6. The comparatively large uncertainties of the derived molecular parameters listed in the lower part of Table 4 mainly reflect the conservative 5% uncertainty which was assumed for the bulk susceptibility.

Table 3. Rotational constants [8], ^{14}N quadrupole coupling constants, molecular g -tensor elements and molecular susceptibility anisotropies of CHF_2CN . Also given are components of the molecular electric quadrupole moment tensor, the so-called paramagnetic susceptibilities, and the anisotropies in the second moments of the electron charge distribution. (Uncertainties correspond to one standard deviation in units of the least significant digit.)

Rotational constants	A	9985.938(51) MHz
	B	4095.116(30) MHz
	C	3081.427(34) MHz
^{14}N quadrupole coupling constants	$\chi_{aa}(^{14}\text{N})$	$-4.3899(33)$ MHz
	$\chi_{bb}(^{14}\text{N})$	$+2.4017(39)$ MHz
	$\chi_{cc}(^{14}\text{N})$	$+1.9883(39)$ MHz
Molecular magnetic g -tensor elements	g_{aa}	$-0.0367(5)$
	g_{bb}	$-0.0350(5)$
	g_{cc}	$-0.0354(3)$
Molecular magnetic susceptibility anisotropies	$2 \cdot \chi_{aa} - \chi_{bb} - \chi_{cc}$	$-13.0(5) \cdot 10^{-6} \text{ erg G}^{-2} \text{ mol}^{-1}$
	$2 \cdot \chi_{bb} - \chi_{cc} - \chi_{aa}$	$+1.6(7) \cdot 10^{-6} \text{ erg G}^{-2} \text{ mol}^{-1}$

Table 4. Molecular parameters which can be calculated from the Zeeman data and additional input such as the structure (Table 5) and the bulk susceptibility (Table 6). In [6] it was shown that the values derived by this method should come close to the corresponding vibronic expectation values. Uncertainties follow from standard error propagation.

Molecular electric quadrupole moments (see Eqs. (6), [5])	Q_{aa}	$-7.9(7)$	$10^{-26} \text{ esu cm}^2$
	Q_{bb}	$+1.4(9)$	$10^{-26} \text{ esu cm}^2$
	Q_{cc}	$+6.5(1)$	$10^{-26} \text{ esu cm}^2$
Paramagnetic susceptibilities (see Eqs. (7), [5])	$\chi_{aa}^{(p)}$	$114.5(2)$	$10^{-6} \text{ erg G}^{-2} \text{ mol}^{-1}$
	$\chi_{bb}^{(p)}$	$281.0(4)$	$10^{-6} \text{ erg G}^{-2} \text{ mol}^{-1}$
	$\chi_{cc}^{(p)}$	$364.0(3)$	$10^{-6} \text{ erg G}^{-2} \text{ mol}^{-1}$
Anisotropies in the second moments of the electronic charge distribution (Eqs. (8), [5])	$\langle 0 \sum_i a_i^2 - b_i^2 0 \rangle$	$38.1(2)$	\AA^2
	$\langle 0 \sum_i b_i^2 - c_i^2 0 \rangle$	$18.8(3)$	\AA^2
	$\langle 0 \sum_i c_i^2 - a_i^2 0 \rangle$	$-56.9(2)$	\AA^2
Diagonal elements of the magnetic susceptibility tensor if referred to the principal inertia axes system	χ_{aa}	$-35.7(19)$	$10^{-6} \text{ erg G}^{-2} \text{ mol}^{-1}$
	χ_{bb}	$-30.9(19)$	$10^{-6} \text{ erg G}^{-2} \text{ mol}^{-1}$
	χ_{cc}	$-27.6(21)$	$10^{-6} \text{ erg G}^{-2} \text{ mol}^{-1}$
Second moments of the electronic charge distribution (see Eq. II.4, Ref. [6])	$\langle 0 \sum_i a_i^2 0 \rangle$	$65.2(8)$	\AA^2
	$\langle 0 \sum_i b_i^2 0 \rangle$	$27.1(8)$	\AA^2
	$\langle 0 \sum_i c_i^2 0 \rangle$	$8.3(8)$	\AA^2

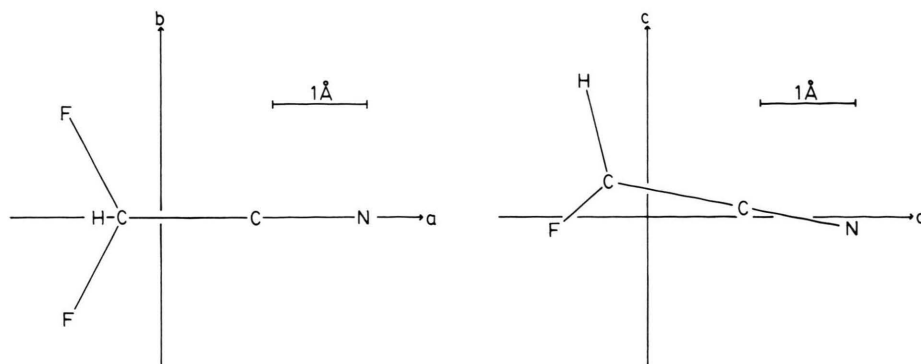


Fig. 3. Partial r_0 structure of difluoroacetonitrile from the work of Ohle and Mäder [9]. The figure shows the orientation of the principal inertia axes system with respect to the nuclear frame in projections on the a, c -plane and on the a, b -plane. Their bond distances are $r_{\text{CH}} = 1.097 \text{ \AA}$, $r_{\text{CF}} = 1.353 \text{ \AA}$, $r_{\text{CC}}^* = 1.460 \text{ \AA}$, and $r_{\text{CN}}^* = 1.158 \text{ \AA}$. Their bond angles are: $\star F\text{CC} = 110.7^\circ$, $\star H\text{CC} = 115.1^\circ$, $\star F\text{CF} = 108.2^\circ$, $\star H\text{CF} = 105.9^\circ$, and $\star \text{CCN}^* = 180.0^\circ$. Values marked with an asterisk have been taken from related molecules. They were held fixed in the least squares fit of the structure to the observed rotational constants.

Table 5. Principal inertia axes coordinates of the atoms in difluoroacetonitrile used to calculate the molecular parameters presented in the lower part of Table 3. They result from the partial r_0 -structure determined by Ohle and may deviate from the true equilibrium structure by up to 0.02 \AA . The $\text{C}-\text{C}\equiv\text{N}$ chain for instance, assumed to be linear by the authors because of the lack of sufficient data, is possibly bent away from the two fluorine atoms by 1 to 3 degrees.

Atom	$a/\text{\AA}$	$b/\text{\AA}$	$c/\text{\AA}$
N	2.173	0.000	- 0.127
C	1.038	0.000	0.099
C	- 0.395	0.000	0.383
H	- 0.656	0.000	1.448
F	- 0.987	- 1.096	- 0.144
F	- 0.987	+ 1.096	- 0.144

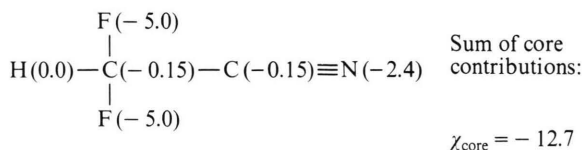
Discussion

In the subsequent discussion we will focus our interest on the interpretation of the molecular magnetic susceptibility tensor as a sum of local contributions [10, 11, 12]. As was the case in acrylonitrile [5], local electronic wavefunctions constructed from delocalized CNDO/2 wavefunctions indicate, that the $\text{C}\equiv\text{N}$ group should be treated as a whole in such a model. (Our rough method to generate localized molecular orbitals has been described in [5], p. 1008.)

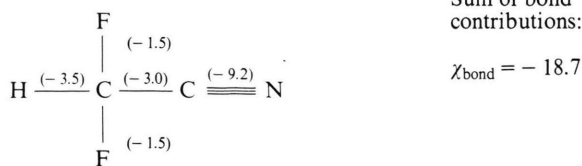
We therefore broke down the observed susceptibility tensor into five local subunits, one for the $\text{C}\equiv\text{N}$ group, one for H-, two for F-, and one for the sp^3 -hybridized central carbon atom.

Table 6. Calculation of the bulk susceptibility of difluoroacetonitrile within the additivity scheme developed by Haberditzel [9]. All values are given in units of $10^{-6} \text{ erg G}^{-2} \text{ mol}^{-1}$. For the C-F contribution we used Haberditzel's $\text{C}(\text{Cl}_2)\text{-F}$ -value as an approximation. The value of -9.2 for the $\text{C}\equiv\text{N}$ -bond is taken from p. 58, Ref. [9]. The other values are taken from the listing on p. 96 and 97 of Ref. [9].

Core contributions



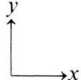
Bond contributions



$$\chi_{\text{bulk}} = (\chi_{aa} + \chi_{bb} + \chi_{cc})/3 = \chi_{\text{core}} + \chi_{\text{bond}} = -31.4$$

From the local susceptibility tensors for H-, F- and for the sp^3 -hybridized central carbon atom (they are given in the upper three rows of Table 7 and were essentially taken from [6], Table II.2), the susceptibility tensor for the nitrile group was obtained in the same way as described in [5]. In two

Table 7. Local susceptibility tensors for the hydrogen, the fluorine and the central "sp³-hybridized" carbon atom essentially taken from Ref. [6], Table II.2 (see text), and the local susceptibility tensor of the nitrile group calculated from the difference between the χ_{aa} , χ_{bb} and χ_{cc} values (Table 4) and those calculated within the additivity scheme from the corresponding local contributions of the HF₂C-frame. Also given for comparison is the nitrile susceptibility tensor determined earlier from a similar study for acrylonitrile. The differences indicate the limits of the simple additivity scheme. Apparently in the case of difluoroacetonitrile electron withdrawal by the electronegative fluorine atoms has diminished the susceptibility contribution from the nitrile region. All values are given in units of 10⁻⁶ erg G⁻² mol⁻¹. — If the nitrile χ -tensor is calculated without the assumption of cylindrical symmetry, the values in brackets are obtained. Here the z-axis would be perpendicular to the molecular symmetry plane.

	χ_{xx}	χ_{yy}	χ_{zz}
H—	− 1.17	− 2.08	− 2.08
F—	− 8.22	− 6.15	− 6.15
H—C $\begin{smallmatrix} \diagup \\ \diagdown \end{smallmatrix}$	− 6.44	− 6.44	− 6.44
—C \equiv N	− 13.9	− 7.32	− 7.32
(this work)		(− 7.36)	(− 7.28)
—C \equiv N [5]	− 21.0	− 12.85	− 12.85

points we deviated slightly from the local susceptibility in [6]:

a) We assumed cylindrical symmetry for the fluorine-carbon bonds and took the average of the χ_{yy} and χ_{zz} -values presented in Table II.2, Ref. [6] for the local fluorine components perpendicular to the bond direction, i.e. we took $\chi_{yy} = \chi_{zz} = -(6.87 + 5.42)/2$ for the fluorine contributions.

b) We assumed spherical symmetry for the local tensor of the central "sp³-hybridized" carbon atom

and tried to account for the electronegative substituents by a linear extrapolation of the averages of the values tabulated for

$$C_{sp^3}(H_3C-) \quad - (9.92 + 8.27 + 8.27)/3, \text{ and}$$

$$C_{sp^3}(H_2C\begin{smallmatrix} \diagup \\ \diagdown \end{smallmatrix}) \quad - (7.45 + 7.19 + 8.26)/3,$$

to a situation where three substituents more electronegative than hydrogen are attached to the carbon atom rather than only one or two.

Our result for the —C \equiv N contribution is tabulated in the fourth row of Table 7. In the fifth row we give the corresponding values determined earlier from the Zeeman data of acrylonitrile.

To us the differences appear to be significant and the decrease in absolute value of the χ -tensor elements attributed to the C \equiv N group when going from acrylonitrile to difluoroacetonitrile appears to be reasonable, since the two fluorine atoms withdraw electron density from the C \equiv N group. However, this in turn could increase the corresponding tensor elements of the F-subunits, an effect which was not yet accounted for in the present analysis because of the lack of sufficient experimental information. In order to get more experimental information on neighbouring bond effects on the local susceptibilities, we plan to study the rotational Zeeman effect of a series of related molecules. The investigation of monofluoroacetonitrile is already in progress.

Acknowledgements

We gratefully acknowledge financial support by Deutsche Forschungsgemeinschaft and the Fonds der Deutschen Chemischen Industrie. The computer calculations were carried out on the PDP-10 computer at the computer center of the Universität at Kiel.

- [1] W. Kasten, H. Dreizler, B. E. Job, and J. Sheridan, *Z. Naturforsch.* **38a**, 1015 (1983).
- [2] W. H. Stolze, M. Stolze, D. Hübner, and D. H. Sutter, *Z. Naturforsch.* **37a**, 1165 (1982).
- [3] K.-F. Dössel and D. H. Sutter, *Z. Naturforsch.* **32a**, 1444 (1977).
- [4] H. D. Rudolph, *Z. Naturforsch.* **23a**, 540 (1968).
- [5] M. Stolze and D. H. Sutter, *Z. Naturforsch.* **40a**, 998 (1985).
- [6] D. H. Sutter and W. H. Flygare, *Topics in Current Chemistry* **63**, 89 (1976).

- [7] W. H. Flygare, *Chem. Rev.* **74**, 654 (1974).
- [8] B. Ohle, Staatsexamensarbeit, Kiel 1984.
- [9] W. Haberditzel, *S.B. Deutsche Akad. Wiss. Berlin. Chem. Geol. Biol.* 1964, Nr. 2.
- [10] T. G. Schmalz, C. L. Norris, and W. H. Flygare, *J. Amer. Chem. Soc.* **95**, 7961 (1973).
- [11] J. Wiese, Diplomarbeit, Kiel 1975.
- [12] Ref. [7], Chapter II.c.